

T1

:

1

: T1

: 42

T1

26

71

1cm

16

10

Gd-

DTPA(0.1mmol/ kg) 3-4cc/sec

10 (

1), 35 (2), 60 (3), 5 ()

: T1

2.873,

3.854

(p>0.01).

1 , 2 , 3 ,

5.565, 3.790, 1.704, 1.282

1

가

3.053, 1.561, 0.919, 1.038

가

1

2.691,

0.801

(p<0.01).

:

T1

T2

(1,2).

T1

T2

가

(3-5).

가

T2

T1

1995 12

1997 3

가

T1 T2

가

T1

42

97 가

(n = 3),

(6-8),

T1

= 13)

1cm

16

12-26

(n

(16)

T1

1cm

10

가

26

1998 11 4

1999 3 6

가

: T1

2.3cm (1.2-2.3cm, mean 1.7cm), 가
 2cm (1.0- 2.0cm, mean 1.4cm).
 (region of interest, ROI)
 1cm

1.5T (Magnetom Vision, Siemens, Erlangen, Germany) spoiled gradient echo technique fast low-angle shot (FLASH) sequence (TR/TE/FA, 113-130/4.1/80,) (chemical shift-selective saturation pulse)

(signal to noise ratio, SNR) 가 four-element phased-array multicoil (magnetic-field homogeneity) (automated shimming) (flow compensation) (gradient motion rephasing, GMR)

Matrix 117-140 x 256 (field of view, FOV) 32-40cm

Gd-DTPA (0.1mmol/kg) (antecubital vein)
 3~4cc/sec
 10 (1), 35 (2), 60 (3),
 5 () 1
 8-10mm , 2mm

12-15 16-19

T1 (nodule-liver contrast-to-noise ratio, CNR)

(background noise standard deviation)
 가
 paired t-test , p 0.01
 가

T1
 2.873, 3.854
 (p > 0.01).

1 , 2 , 3 ,
 5.565, 3.790, 1.704, 1.282 (Table 1). 16
 14 (87.5%) 1 가
 (Fig. 1),

2 2
 3.053, 1.561, 0.919, 1.038 (Table 1). 10
 9 (90%)
 가 (Fig. 2). 1

2.691, 0.801 1
 가 1

$$CNR = \frac{S_n - S_l}{noise\ SD}$$

Sn : signal intensity of the nodule, Sl : signal intensity of surrounding liver parenchyma, noise SD : standard deviation of the intensity of background noise in the phase encoding direction

Table 1. Mean Contrast to Noise Ratio of Hepatocellular Carcinoma and Dysplastic Nodule

	Mean CNR				
	Pre	Phase 1	Phase 2	Phase 3	Delay
HCC	2.873	5.565	3.790	1.704	1.282
DN	3.854	3.053	1.561	0.919	1.038

CNR : contrast to noise ratio, HCC : hepatocellular carcinoma, DN : dysplastic nodule

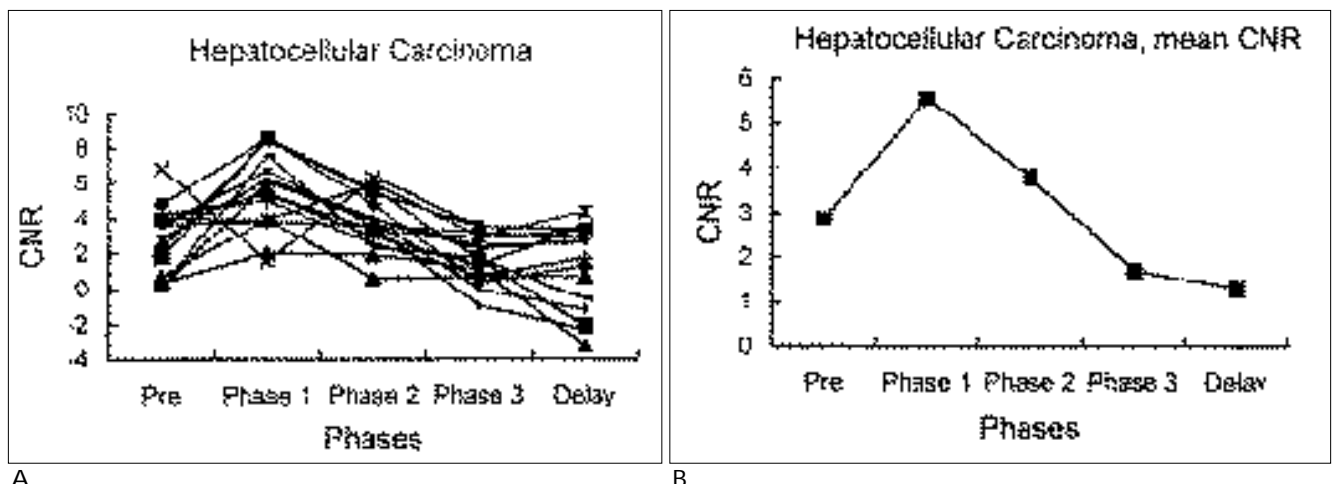
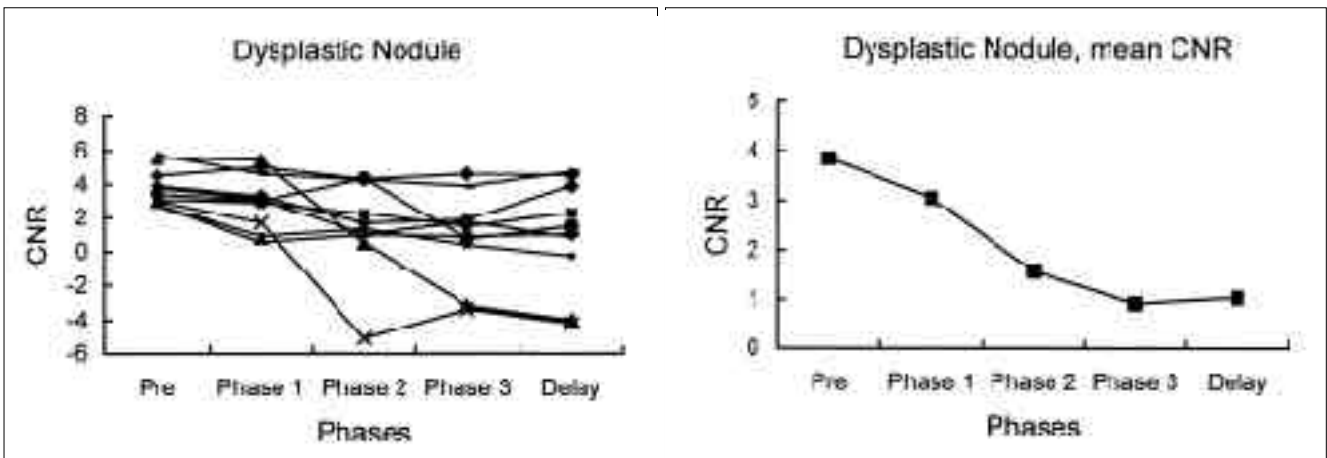


Fig. 1. The CNR versus phase of small hepatocellular carcinoma. This figure shows CNR of 16 small hepatocellular carcinomas (A) and the mean CNR curve (B). Small hepatocellular carcinoma showed peak CNR at phase 1 after contrast injection due to early contrast uptake of the tumor. In the following phases, the CNR of small hepatocellular carcinoma rapidly decreased.

(p < 0.01).

(1,2). T2 (6-8). 가 (13,14). T2 가 (4,5,9). Edmondson 2 가 (Fig. 3). 16 T2 Edmondson 1 가 가 6 (37.5%), 3 가 10 가 3 가 3 T2 T1 (Fig. 3). 6 (37.5%) (1,3,4,10-12). (clear cell) (glyco- gen) 가 (14/16, 87.5%) 가 (9/10, 90%) T1 가 (1,2), 가 가 (11). (protocol) T1 가 가 2 가 1



A B
 Fig. 2. The CNR versus phase of dysplastic nodule. This figure shows CNR of 10 dysplastic nodules (A) and the mean CNR curve (B). Dysplastic nodule showed no peak CNR at phase 1 compared to small hepatocellular carcinoma. The CNR in subsequent phases gradually decreased.

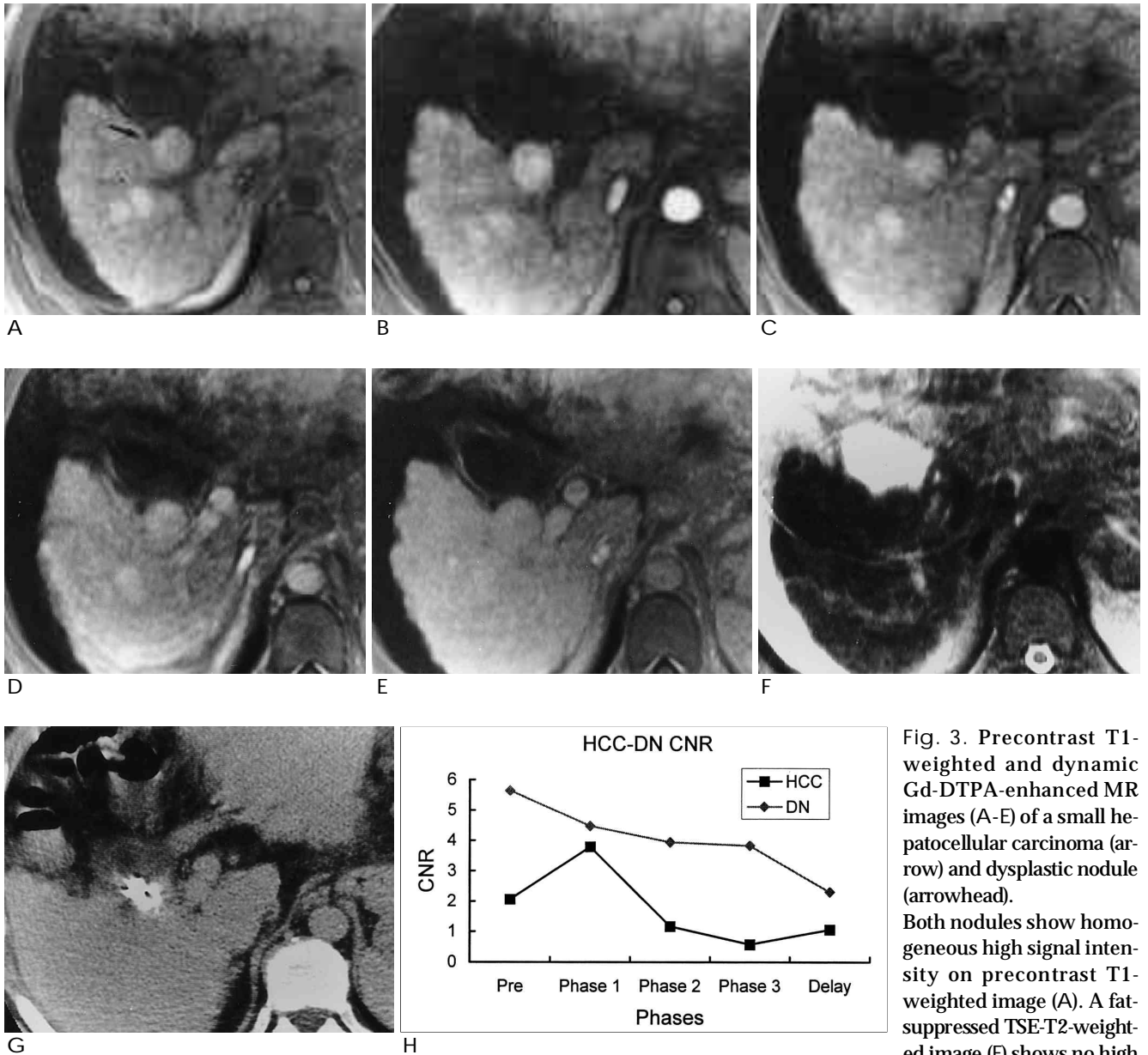


Fig. 3. Precontrast T1-weighted and dynamic Gd-DTPA-enhanced MR images (A-E) of a small hepatocellular carcinoma (arrow) and dysplastic nodule (arrowhead). Both nodules show homogeneous high signal intensity on precontrast T1-weighted image (A). A fat-suppressed TSE-T2-weighted image (F) shows no high signal intensity for these nodules. The degree of visual enhancement is not overt on dynamic study (B-D) and there is no contrast wash-out or capsular enhancement on delayed image (E). However, the CNR versus phase curve shows a rapid increase in CNR at phase 1 in small hepatocellular carcinoma (H) correlated with lipiodol CT scan (G) and no peak of CNR in dysplastic nodule (H).

(8,15).

가

가 1
(circulation time)

(8,15),

가

가

2

(16-18).

1

1

가

(19),

16

가

3 23
 1 (12-26 16)
 3-4 3-6 2-3
 (19, 20).

T1

1. Ebara M, Ohto M, Watanabe Y, et al. Diagnosis of small hepatocellular carcinoma : correlation of MR imaging and tumor histologic studies. *Radiology* 1986;159:371-377
2. Matsui O, Kadoya M, Kameyama T, et al. Adenomatous hyperplastic nodules in the cirrhotic liver : differentiation from hepatocellular carcinoma with MR imaging. *Radiology* 1989;173:123-126
3. Ebara M, Watanabe S, Kita K, et al. MR imaging of small hepatocellular carcinoma : effect of intratumoral copper content on signal intensity. *Radiology* 1991;180:617-621
4. Kadoya M, Matsui O, Takashima T, Nonomura A. Hepatocellular carcinoma : correlation of MR imaging and histopathologic findings. *Radiology* 1992;183:819-825
5. Inoue E, Kuroda C, Fujita M, et al. MR features of various histological grades of small hepatocellular carcinoma. *J Comput Assist Tomogr* 1993;17:75-79
6. Mirowitz SA, Lee JKT, Butierrez E, et al. Dynamic gadolinium-enhanced rapid acquisition spin echo MR imaging of the liver. *Radiology* 1991;179:371-376
7. Ito K, Choji T, Nakada T, et al. Multislice dynamic MRI of hepatic tumors. *J Comput Assist Tomogr* 1993;17:390-394
8. Yamashita Y, Fan ZM, Yamamoto H, et al. Spin echo and dynamic gadolinium-enhanced FLASH MR imaging of hepatocellular carcinoma : correlation with histopathologic findings. *J Magn Reson Imaging* 1994;4:83-90
9. Inoue E, Kuroda C, Narumi Y, et al. Magnetic resonance imaging-histologic correlation of small hepatocellular carcinomas and adenomatous hyperplasias. *Invest Radiol* 1993;28:691-697
10. Muramatsu Y, Nawano S, Takayasu K, et al. Early hepatocellular carcinoma : MR imaging. *Radiology* 1991;181:209-213
11. Mitchell DG, Palazzo J, Hann H-WYL, Rifkin MD, Burk DL Jr, Rubin R. Hepatocellular tumors with high signal on T1-weighted MR images : chemical shift MR imaging and histologic correlation. *J Comput Assist Tomogr* 1991;15:762-769
12. Bartolozzi C, Lencioni R, Caramella D, et al. Correlations between magnetic resonance imaging and histopathologic findings in hepatocellular carcinoma. *Radiol Med* 1994;87:90-95
13. Yamashita Y, Hatanaka Y, Yamamoto H, et al. Differential diagnosis of focal liver lesions : role of spin-echo and contrast-enhanced dynamic MR imaging. *Radiology* 1994;193:59-65
14. Yamashita Y, Mitsuzaki K, Yi T, et al. Small hepatocellular carcinoma in patients with chronic liver damage : prospective comparison of detection with dynamic MR imaging and helical CT of the whole liver. *Radiology* 1996;200:79-84
15. Ikeda K, Saitoh S, Koida I, et al. Diagnosis and follow-up of small hepatocellular carcinoma with selective intraarterial digital subtraction angiography. *Hepatology* 1993;17:1003-1007
16. Matsui O, Kadoya M, Kameyama T, et al. Benign and malignant nodules in cirrhotic livers : distinction based on blood supply. *Radiology* 1991;178:493-497
17. Park YN, Yang CP, Fernandez GJ, Cubukcu O, Thung SN, Theise ND. Neovascularization and sinusoidal capillarization in dysplastic nodules of the liver. *Am J Surg Pathol* 1998;22:656-662
18. Krinsky GA, Theise ND, Rofsky NM, Mizrachi H, Tepperman NW, Weinreb JC. Dysplastic nodules in cirrhotic liver: arterial phase enhancement at CT and MR imaging a case report. *Radiology* 1998;209:461-464
19. Takayama T, Makuuchi M, Hirohashi S, et al. Malignant transformation of adenomatous hyperplasia to hepatocellular carcinoma. *Lancet* 1990;336:1150-1153
20. Theise ND. Macroregenerative (dysplastic) nodules and hepatocarcinogenesis : theoretical and clinical considerations. *Semin Liver Dis* 1995;15:360-371

Focal Hepatic Nodules with High Signal Intensity on T1-weighted MR Imaging : Differentiation of Small Hepatocellular Carcinoma from Dysplastic Nodule by Quantitative Analysis of Multi-phase Contrast-enhanced Dynamic MR Imaging¹

Kwang-Hun Lee, M.D., Jeong-Sik Yu, M.D., Ki Whang Kim, M.D., Nariya Cho, M.D.,
Mi-Gyoung Jeong, M.D., Jai Keun Kim, M.D.

¹Department of Diagnostic Radiology, Research Institute of Radiological Science, Yonsei University College of Medicine, Seoul, South Korea

Purpose : To evaluate the usefulness of quantitative analysis of the degree of enhancement in dynamic MR imaging used to differentiate dysplastic nodule (DN) from small hepatocellular carcinoma (HCC), both of which show high signal intensity on T1-weighted images.

Materials and Methods : From 26 small HCCs and 71 DNs, all of which showed homogeneous high signal intensity on T1-weighted images among 42 patients with liver cirrhosis, we selected 16 small HCCs and 10 DNs of more than 1cm in diameter which were diagnosed by biopsy and follow-up imaging. Dynamic MR imaging of the entire liver was obtained using the breath-hold technique at postinjection 10 sec. (phase 1), 35 sec. (phase 2), 60 sec. (phase 3), and 5 min. (delayed) after intravenous manual injection of Gd-DTPA (0.1 mmol/kg) at a velocity of 3-4 cc/sec. Nodule-to-liver contrast-to-noise ratios (CNR) during each phase were calculated by measurement of the region of interest.

Results : On precontrast T1-weighted images, the mean CNR of small HCCs was 2.873, and that of DNs was 3.854, there was thus no significant statistical difference ($p > 0.01$). On postcontrast images, the CNR of small HCCs during each phase was 5.565, 3.790, 1.704, and 1.282, with peak CNR phase 1 and a mostly decreasing trend thereafter. However, the CNR of DNs during each phase was 3.053, 1.561, 0.919, and 1.038 ; there was thus showed no significant increase during phase 1 in comparison with the CNRs seen on precontrast images. During the precontrast stage and phase 1, the average difference in CNR was 2.691 for small HCCs and 0.801 for DNs the difference was thus significant ($p < 0.01$).

Conclusion : Quantitative analysis of CNR, reflecting the degree of nodule-to-liver enhancement in dynamic MR imaging, was found to be useful for the differentiation of small HCCs from DNs, both of which show high signal intensity on T1-weighted images.

Index words : Liver, neoplasms
Liver, MR

Address reprint requests to : Jeong-Sik Yu, M.D., Department of Diagnostic Radiology, Yonsei University College of Medicine, YongDong Severance Hospital, #146-92 Dokok-Dong, Kangnam-Ku, Seoul, 135-270, South Korea.
Tel . 82-2-3497-3510 Fax . 82-2-3462-5472 E-mail. yjsrad97@yumc.yonsei.ac.kr